ITC 3/53
Information Technology and Control
Vol. 53 / No. 3/ 2024
pp. 916-931
DOI 10.5755/j01.itc.53.3.36925

Preclinical Computer Virtual Reduction of Fracture Surgical Robot Based on Iterative Closest Point Algorithm

Received 2024/04/08 | Accepted after revision 2024/05/29

HOW TO CITE: Zhang, X., Qian, J., Mao, Y., Zhang, Y., Ye, J., Xun, Y., Yang, Q. (2024). Preclinical Computer Virtual Reduction of Fracture Surgical Robot Based on Iterative Closest Point Algorithm. *Information Technology and Control*, 53(3), 916-931. https://doi.org/10.5755/j01.itc.53.3.36925

Preclinical Computer Virtual Reduction of Fracture Surgical Robot Based on Iterative Closest Point Algorithm

Xinxing Zhang
College of Mechanical Engineering, Zhejiang University of Technology, Hangzhou, China
Key Laboratory of Special Purpose Equipment and Advanced Processing Technology, Ministry of Education and Zhejiang Province, Zhejiang University of Technology, Hangzhou, China
Department of Mechanical and Electrical Engineering, Quzhou College of Technology, Quzhou, China

Jun Qian
Department of Orthopedics, People's Hospital of Quzhou, The Affiliated Hospital of Wenzhou Medical University, Quzhou, China

Yunsheng Mao
College of Mechanical Engineering, Zhejiang University of Technology, Hangzhou, China
Key Laboratory of Special Purpose Equipment and Advanced Processing Technology, Ministry of Education and Zhejiang Province, Zhejiang University of Technology, Hangzhou, China

Yingqi Zhang
Department of Orthopedics, Tongji Hospital, School of Medicine, Tongji University, Shanghai, China

Juncai Ye
Department of Orthopedics, Zhejiang Hospital, Hangzhou, China

Yi Xun
College of Mechanical Engineering, Zhejiang University of Technology, Hangzhou, China
Key Laboratory of Special Purpose Equipment and Advanced Processing Technology, Ministry of Education and Zhejiang Province, Zhejiang University of Technology, Hangzhou, China

Qinghua Yang
College of Optical, Mechanical and Electrical Engineering, Zhejiang A & F University, Hangzhou, China
College of Mechanical Engineering, Zhejiang University of Technology, Hangzhou, China

Corresponding author: Qinghua Yang, robot@zjut.edu.cn; Yi Xun, xunyi@zjut.edu.cn

Reduction is a crucial stage in the surgical treatment of bone fractures. The detailed fracture information of the patient can be obtained from computed tomography (CT) scans before surgery and enable physicians to plan preoperative reduction, to reduce the operation time and thus increase the probability of getting satisfactory results. The primary purpose of this paper is to design a computer-aided automatic registration method of fracture point cloud data, so as to simplify the fracture reduction process. In this paper, we propose an integrated fracture reduction system was introduced. The system enables direct semi-automatic processing from CT images to fracture reduction. First, a 3D fracture models is reconstructed from CT images by using the modified Marching Cube (MC) algorithm and is discretized to generate a point cloud. Second, the K-dimensional (KD) tree algorithm is used to cluster and segment the point clouds to identify different fracture fragments. Last, through the combination algorithm of Normal Distributions Transform (NDT) and modified Iterative Closest Point (ICP), the coarse alignment and fine registration of point clouds are achieved step by step. This method has been successfully applied to the reduction of tibial fracture. In the tests performed, the processing time of each step, the point cloud and the 3D model after registration are displayed. The semi-automatic integrated system based on preoperative CT scanning is used to realize fracture reduction, which provides a feasible foundation for minimally invasive and accurate fracture reduction surgery.

KEYWORDS: Computer-assisted preoperative planning, Bone reduction, Point cloud, Bone registration, Iterative closest point (ICP) algorithm, Surgical robot

1. Introduction

People of all ages are at risk of fractures, especially the long bones of the human limbs play an essential role in our lives as levers for human movement. Fractures are a common type of bodily injury, and most patients can recover with timely and appropriate treatment. However, due to the unreasonable treatment process, some patients may suffer delayed fracture healing, fracture nonunion, infection, and other surgical complications. In fracture treatment, reduction, fixation, and training are three essential stages.

We focus on the fracture reduction stage, and the other two stages are outside the scope of this study. The computer simulation process of preoperative 3D fracture reduction is mainly divided into four steps: reconstruction of 3D fracture model, identification of fracture fragments, registration of fracture fragments and analysis of results [20, 11, 10].

Three-dimensional model reconstruction has the advantage of intuitively and accurately representing the patients' skeletons and is widely used in orthopedic diagnosis, surgical planning, training and learning, surgery simulation, and implant selection [21].

Effective identification of fractured areas allowed for a better understanding of patient fractures and obtained a clear division of the fracture boundary, which involved the segmentation of bone fragments. In the previous literature, the proposed reduction method is usually by extracting some feature points in the fracture area or by interaction for registration at a later stage [3, 4]. This feature information can be used for repositioning based on the distance minimization algorithm, thus improving the reduction result [28, 26, 29, 25, 19, 13].

In previous work, different methods have been proposed for fracture reduction. Several works propose the reduction of fractures by computing, matching, and recording fracture areas. Other works design human-computer interaction tools or use the healthy contralateral bone as a reference during fracture reduction. The following introduction analyzes the most relevant jobs and discusses main merits and drawbacks of each approach.

2. Related Work

Several human-computer interaction methods have been proposed to extract contour information from craniofacial fracture regions. Chowdhury et al. [4] proposed a computer 3D reconstruction method for mandibular multi-segment fractures based on CT image sequences. The maximum weight mapping matching algorithm identified the fracture surface, and then the corresponding fracture surface was registered by the iterative closest point (ICP) algorithm. Chowdhury et al. [6] extended this work and proposed a variant of this method, which is used to establish the corresponding relation of a given fracture surface to optimize the calculation of the nearest point in the ICP algorithm. Constraints derived from the volume

matching process continuously monitor the performance of 3D reconstruction.

The method devised by Winkelbach et al. [28] is suitable for reducing cylindrical fragments. However, it cannot be used when the fracture is not in the diaphyseal region, or the fracture line is approximately parallel to the bone axis. Winkelbach et al. [27] developed this approach to the automatic registration of bone fragments of arbitrary form. An effective Random Sample Consistency (RANSAC) algorithm is presented, which estimates the attitude and evaluates the matching quality by randomly selecting a pair of points. The algorithm is executed iteratively until a good match is obtained. However, the user needs to define additional constraints, which is often difficult because some prior knowledge is required.

Willis et al. [26] presented a reconstruction technique for comminuted fractures of long bones based on statistical methods. In this approach, binary classification is performed using a hybrid model consisting of two Gaussian probability distributions, allowing the separation of intact and fractured regions of each bone fragment. This method requires manual identification of possible corresponding fracture surfaces and automatic alignment of bone fragments with a modified ICP algorithm, which was tested in a single tibial fracture case, but accuracy was not assessed.

Zhou et al. [29] selected a two-class Bayesian classifier that realized the separation of broken and intact surfaces based on the intensity value at the vertex of the surface. The performance of this algorithm is validated in a clinical tibial plateau case obtained from CT and several artificial fractures based on bone replicas.

Moghari and Abolmaesumi [17] proposed a technique for automatically registering multiple bone fragments of fractures, a global registration method guided by the statistical anatomical atlas model. Using the local point descriptor, the fracture fragments are initially aligned with the generated atlas. This local point descriptor is robust to identify a group of potential corresponding points between the fragments and the mean atlas model. Then the global registration algorithm is used to fine-tune the alignment between the fractures and the mean atlas model. The proposed global alignment method showed high precision in a cadaver study, but collecting anatomical atlas models will be a significant challenge.

Okada et al. [18] proposed a reduction plan for femoral head fracture based on three-dimensional curvature analysis, which uses the following three constraints: contra-lateral bone, fracture surface, or fracture surface constrained by the contra-lateral bone. The disadvantage of this method is that when multiple interconnected fragments are obtained through simple CT image threshold processing, the surgeon needs to separate each bone fragment manually. However, this process is often terminated due to noise interference, CT resolution, and other factors.

Fürnstahl et al. [6] proposed a computer-aided method to quantify the critical displacements affecting a successful joint repair. Bone reconstruction is achieved by multi-segment alignment. In case of large displacement, the reconstruction template based on the reference humerus is included in the algorithm to calculate the best match. The main disadvantage is that it requires extensive manual matching and parameter selection at several stages of the algorithm, which is a complex and time-consuming task.

Kronman and Joskowicz [12] proposed a method for automatically reducing fracture models. The algorithm identifies the fracture contact surface based on the maximum principal curvature of the fragment surface and its intensity distribution in CT scanning. Then, the two fracture surfaces are aligned by rigid registration to obtain virtual fracture reduction. The problem is the lack of clinical cases.

Buschbaum et al. [2] created virtual three-dimensional bone fragments from CT scanning. According to the calculated surface curvature, strongly curved edges are selected, and fracture lines are generated. After assigning matching points, compare these fracture lines and calculate the desired target location. The experimental datasets are derived from artificial bone models and cannot be directly applied to clinical cases obtained from medical images.

Paulano-Godino and Jimenez-Delgado [19] proposed an automatic method for calculating the contact area between two bone fragments and matching bone fragments in complicated fractures. The fracture reduction process of multiple fragments can be simplified to the reduction of numerous paired fragments, and the reduction order depends on the value of the automatic matching function.

Vlachopoulos et al. [24] presented a novel approach for reconstructing fractures in the proximal humerus.

The core idea of this method is to match features between fragments through a scale-space curvature, allowing calculations based on the corresponding area of the fracture line to achieve the correct alignment between bone fragments. Their methods use manual breakpoint annotation, increasing the running time of the algorithm.

Liu et al. [13] proposed a semi-automatic method framework to provide technical support for customized precision medicine. This reduction takes advantage of the cylinder-like characteristics of the long bone shaft. It is achieved by eliminating large deviations from the curvature and the normal of the bone axis. Because the experiment used an artificial bone model, applying it to clinical cases is challenging.

Han et al. [7-9] proposed a single bone fracture reduction plan based on statistical shape model (SSM) volume representation and a pelvic dislocation reduction plan based on statistical pose model (SPM). After that, a unified model combining SSM and SPM is established, and fracture reduction planning under the multi-bone background is proposed. As far as we know, this is the first work to solve the restoration planning in the context of multiple bones, including the description of bone shape and pose. Compared with point registration, this method solves the problems in the volume image domain, thus avoiding the definition of point correspondence, and uses operations between objects (such as intersection and union) to achieve better registration regularization. The multi-body registration framework has been successfully applied to various simulation and clinical scenarios requiring user interaction.

Deng et al. [5] presented a semi-automatic data-driven method. A deep neural network was used to generate synthetic training data, and the final reduction position of the fracture was obtained through iterative axis alignment and position alignment, and the results were compared with the ICP algorithm.

Luque-Luque et al. [15] proposed a fracture reduction method that can be applied to all kinds of bones and regions. It identified the intact fracture region and adopted the improved iterative closest point algorithm to deal with the distance between fragments. This method can deal with large cracks and process complicated or deformed fragments. No specific region or case has been considered, so all possible cases and situations must be obtained and proven.

Arumugam et al. [1] presented a method of virtual bone reduction and reconstruction for comminuted pelvic fractures using CT scan data set. This included segmentation, 3D model optimization and ICP bone registration techniques. The accuracy of the reconstructed bone model was verified by finite element method.

From the above work on fracture reduction, we summarize some problems that need to be solved. These include automating the reduction process or minimizing human-computer interaction, conducting experiments with real rather than simulated data, and developing registration methods that do not rely on the contra-lateral bone. We propose a new integrated computer-aided system that includes reconstructing a 3D fracture bone model using sequential CT images, generating and segmenting point cloud data of the fracture area, and registering the point cloud. The aim & scope of the study is to presents an approach that attempts to minimize surgeon intervention as much as possible, making it closer to an automated approach whose sub-steps are mostly mature (stable) algorithms. The method, which identifies intact fracture areas and uses an improved ICP algorithm to deal with the distance between fragments, can be applied to fractures in the long shaft region.

The major novelty and contribution of this paper include:

- The algorithm does not include the extraction of feature points, which is often used in previous algorithms and increases the complexity of the algorithm;
- There is no need to use healthy contralateral bone, avoiding the scanning of healthy bone and reducing the damage to the patient;
- Improved ICP algorithm and KNN method were used to cluster and segment fracture point cloud data;
- The whole process is semi-automatic, finding the right balance between manual and automatic to minimize unnecessary human-computer interaction.

The structure of this paper is as follows. Section 2 describes the experimental data, the software, and the proposed fracture reduction algorithm. Section 3 introduces the technical application and experimental

results in different stages of fracture reduction. Section 4 analyzes and compares the capabilities of the algorithms, as well as their limitations and shortcomings. In the last chapter, the completed work is summarized, and the future direction of work has prospected.

3. Methodology

3.1. Ethics Statement

The study was approved by the Ethics Committee of the People's Hospital of Quzhou (ethical identification number 075/2022). The responsibilities, composition, operating procedures and records of this Ethics Review Committee are in accordance with the Biological Medicine Involving People Methods for Ethical Review of Scientific Research, International Ethical Guidelines for Health-related Research Involving Humans, Declaration of Helsinki, Good Clinical Practice (GCP) and Guideline for Good Clinical Practice of the International Conference on Harmonisation (ICH-GCP), and relevant domestic laws and regulations. The list of documents reviewed by the Ethics Committee includes: (1) Application Form for Ethics Review; (2) Research plan; (3) Informed consent for exemption application.

This paper reports a study of archived samples. All data were completely anonymous and the Ethics Committee waived the requirement of informed consent and agreed to use the data in the patient's medical records in the study, mainly including the data from the CT examination of bone fractures. The archived samples were collected in 2016, and the date of this study was September 9, 2022. Authors do not have access to information that identifies individual participants during or after data collection. The study did not involve vulnerable groups, no potential harm to the study participants, no invasive procedures, and all procedures were manually signed by the principal applicant.

3.2. Materials and Methods

Our experiment selected the CT image data of tibial fractures from patient. Dedicated software for this application was developed using the C++ programming language (Visual Studio 2019, Microsoft, Redmond, WA), with Qt 5.15.2 for GUI programming (Nokia, Oslo, Norway), the Visualization ToolKit (VTK 9.0) for visualization in 3D. Point Cloud Library (PCL 1.9.1) is a standalone, large-scale, open project in segmentation and registration for 2D/3D image and point cloud processing.

This section proposes an improved algorithm for the segmentation and registration of broken bone point clouds, which provides a feasible technical solution for the preoperative planning of fractures. The proposed method mainly consists of three stages. Firstly, the 3D fracture model is reconstructed from CT by an improved MC algorithm and discretized to generate a point cloud. Secondly, the KD-tree algorithm clusters and segments the point clouds to identify different fracture bones. Finally, the normal distributions transform (NDT) algorithm is used for coarse alignment [16], and the improved iterative closest point (ICP) algorithm is used for fine registration. In addition to some necessary parameters such as fracture Angle, bone Hounsfield strength threshold need to be input, all sub-steps can be set as automatic (non-manual) processing, which effectively improves the automation degree of the system.

3.3. 3D Reconstruction of Fracture Model

Three-dimensional fracture reconstruction refers to modeling the displacement of bone fragments in the fracture area and the size of the fragments through CT images after a fracture. Doctors can observe fracture information from three-dimensional structures and make surgical plans. Two-dimensional x-rays are generally taken after fractures, but some occlusions are not conducive to our observation and acquisition of complex fracture information.

There are generally four categories for 3D reconstruction using CT images: surface fitting, contour skinning, volume polygonization, and implicit function interpolation. Our application uses a fast and simple Marching Cubes algorithm based on volumetric polygonization, which allows the high-resolution generation of large polygon datasets from volumetric data. However, this algorithm requires high computational costs, and the generated isosurfaces may have holes due to ambiguity. The proposed application can handle surfaces with holes by setting multiple isosurface values. The detailed steps of the improved marching cube algorithm can be found in the reference [22].

The main processes of this part of the work were as follows: First, the fractured bone's cross-sectional image was obtained from the CT machine and then

imported into the computer. Secondly, the section information of the CT image was read through the Visualization ToolKit (VTK), and the necessary parameters were determined. Then three-dimensional reconstruction was implemented by the improved MC algorithm, which approximated the isosurface by a linear difference in the 3D discrete data field. We define a threshold in medical image segmentation and reconstruction to determine this isosurface. The flowchart of the three-dimensional reconstruction in this study is shown in Figure 1. During the reconstruction process, the points cloud data of the bones were acquired as training data for identifying and registering bone fragments in the following sections.

Figure 1
Flowchart of 3D Image Reconstruction

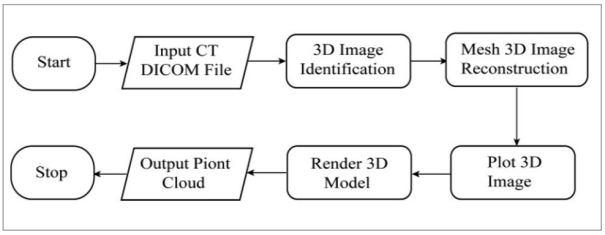

3.4. Fracture Bone Identification

It is essential to identify the fracture area information in fracture treatment. The higher the recognition accuracy of the fracture area, the better the result will be. However, this complex process requires not only segmentation of the bone tissue but also dealing with faulty connections of fragments, so prior knowledge is often needed. While implementing automated procedures is not always possible, user interaction should be minimized as this saves surgical time. We propose a k-nearest neighbor (KNN) based method to identify point clouds of skeletal fragments. For simplicity, we take the segmentation of the first two bone fragments as an example. To split multiple bone fragments, repeat the process.

When implementing the KNN method, the primary consideration is performing a fast k-nearest neighbor search for the point cloud data (as described above), which is especially important when the feature space dimension is large, and the point cloud data capacity is large. The simplest implementation of the k-nearest neighbor method is a linear scan. At this time, the distance between the input and training instances needs to be calculated. When the training set is large, the calculation is time-consuming, and this method is not feasible.

In the implementation of the KNN method, as mentioned above, how to perform a fast KNN search on point cloud data is the priority, which is more important when the dimension of feature space and the capacity of point cloud data are large. The simplest implementation of the KNN method is linear scanning, which is usually applied to smaller training sets. For large training sets, this approach is computationally time-consuming and infeasible. The method based on Kd-tree is used to improve the efficiency of the K-nearest neighbor search. The specific implementation is as follows: assuming that the point cloud of the i-1 layer is the source point cloud, search for the points closest to the upper layer in the current i layer, and judge the search result. If the number of point clouds is unique, it is the same bone as the upper layer. The flowchart of fracture bone identification in this study is shown in Figure 2. The proposed KNN is summarised in Algorithm 1. This representation allows us to do fast searches in an optimized way, which reduces runtime.

Figure 2
Flowchart of fracture bone identification

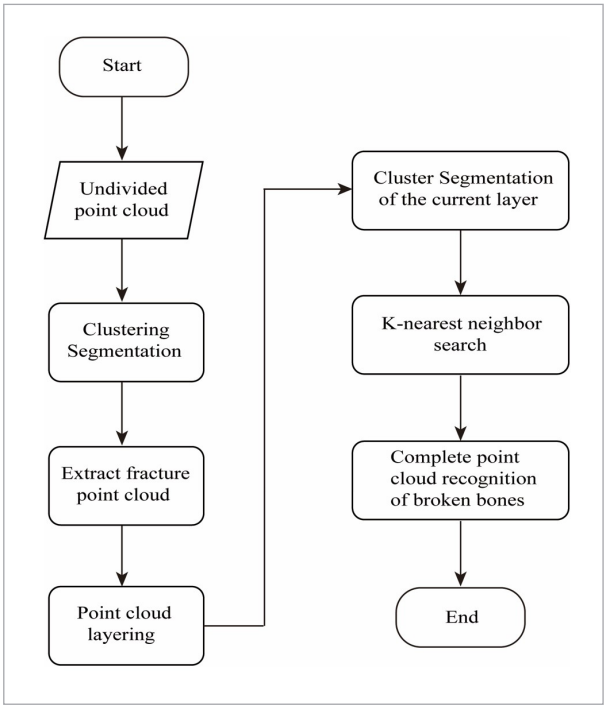

Algorithm 1. KNN, returning the closest point to point p_i in the subtree rooted at node N.

KD-nn-search $\left(p_i, N\right) \Rightarrow \left(q_i, r_i, done\right)$
Require: *p_i is query point and N is the root of the tree in which to search. Each internal node N stores two sub-nodes N_{left} and N_{right}, as well as an index k_n that specifies the dimension along which N splits the space, and a scalar d_n that determines the split point between the two sub-trees.*
Ensure: *q_i is the nearest neighbor of query point p_i, r_i is the distance between the point p_i and the point q_i, done is true if the closest neighbor point has been found.*

if N is leaf node **then**
  $q_i \leftarrow \text{argmin}_{q_i} \left\| p_i - q_i \right\|$
  $r_i \leftarrow \left\| p_i - q_i \right\|$
else $\{N$ is an internal node$\}$
  $d \leftarrow p_i\left[k_n\right] - d_n$
  if $d < 0$ **then**
    $\left(q_i, r_i, done\right) \Leftarrow kd\text{-}nn\text{-}search\left(p_i, N_{left}\right)$
  else
    $\left(q_i, r_i, done\right) \Leftarrow kd\text{-}nn\text{-}search\left(p_i, N_{right}\right)$
  end if
  if *done* $\neq$ *true* **then** *{Backtracking}*
    if $d < 0$ **then** *{Bounds-overlap-ball test:}*
      if *the sphere centred at p_i with radius r_i overlaps N_{right}* **then**
      $(q_i^{'}, r_i^{'}, done) \Leftarrow kd\text{-}nn\text{-}search\left(p_i, N_{right}\right)$
      end if
    else
      {Bounds-overlap–ball test:}
      if *the sphere centred at p_i with radius r_i overlaps N_{left}* **then**
      $(q_i^{'}, r_i^{'}, done) \Leftarrow kd\text{-}nn\text{-}search\left(p_i, N_{left}\right)$
      end if
    end if
    if $r_i^{'} < r_i$ **then**
      $q_i \leftarrow q_i^{'}$, $r_i \leftarrow r_i^{'}$
    end if
  end if
end if
{Bounds-overlap–ball test:}
if *r > distance from p_i to closest boundary to N* **then**
  return $\left(q_i, r_i, \text{false}\right)$
else
  return $\left(q_i, r_i, \text{true}\right)$
end if

3.5. Registration of Bone Fragments

The purpose of bone reduction is to restore the fractured bone segment to its original anatomical position. Our method's computing strategy for bone fracture reduction combines NDT and a modified ICP algorithm. ICP is a commonly used method with high accuracy in three-dimensional fracture registration. The method needs to provide a good initial value when running, that is, rough alignment. Due to the defects of the algorithm itself, the final iterative result may fall into a local optimum, and the registration speed is slow, which cannot achieve the desired effect. NDT is a coarse alignment method based on orthogonal distribution changes, which determines the optimal matching between two point clouds through standard optimization technology. Since there is no need to calculate and match the corresponding points in the alignment process, the advantage is that the processing time is relatively fast, and the disadvantage is that the accuracy is relatively low. Therefore, this paper proposes a combination of NDT and an improved ICP algorithm to improve the accuracy and speed of registration. First, the NDT algorithm is used for rough alignment to obtain transformation parameters, and then the modified ICP algorithm combines the transformation parameters for fine registration.

The main framework of the NDT algorithm for the rough alignment of point clouds is as follows: (1) The acquired fracture point cloud data is divided into several three-dimensional cubes of uniform size, and each cube contains a certain number of points. (2) Point clouds follow Gaussian distribution in the cube, and the mean value and covariance matrix of Gaussian distribution parameters of fracture point cloud data is obtained. (3) The discrete fracture point cloud is represented piecewise in the form of probability density, and the representation is required to be continuous and differentiable. (4) Use the Hessian matrix to minimize the probability density function to obtain the transformation matrix.

ICP is one of the most classic data processing algorithms. The framework of the method is as follows: firstly, the matching point pairs between the source point cloud and the target point cloud are obtained; secondly, the weight of the matching point pairs is allocated according to the needs, and the transformation matrix is constructed for the matching point pairs; thirdly, the source point cloud is matched to the

target point cloud by the transformation matrix; and finally, the error of the transformed point cloud data is estimated by iterative operation until the error-index meets the given requirements.

In the research of [14, 23], a new variant of the ICP algorithm is obtained by modifying the following two parameters: (1) Error metric from point to plane instead of point to point. (2) Linear least square method is used to approximate the nonlinear optimization problem. The distance measurement from point to plane is shown in Figure 3.

Figure 3

The point-to-plane error metric between two surfaces

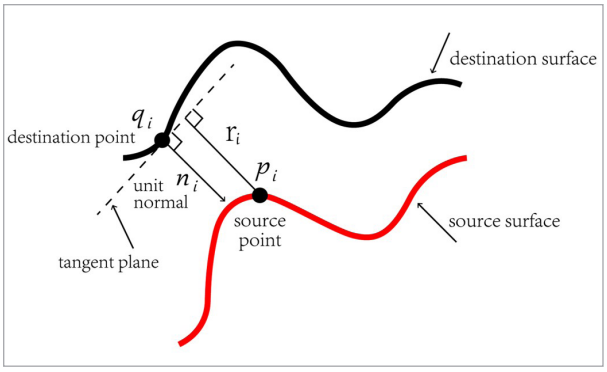

More specifically, if $p_i = (p_{ix}, p_{iy}, p_{iz}, 1)^T$ is a source point, $q_i = (q_{ix}, q_{iy}, q_{iz}, 1)^T$ is the corresponding destination point, $n_i = (n_{ix}, n_{iy}, n_{iz}, 0)^T$ is the unit normal vector at q_i, then the goal of each ICP iteration is to find M_{opt} such that

$$M_{opt} = \arg\min_M \sum_i ((M \bullet p_i - q_i) \bullet n_i)^2, \quad (1)$$

where M and M_{opt} are 4×4 3D rigid-body transformation matrices. A 3D rigid-body transformation M is composed of a rotation matrix $R(\alpha, \beta, \gamma)$ and a translation matrix $T(t_x, t_y, t_z)$, *i.e.*

$$M = T(t_x, t_y, t_z) \bullet R(\alpha, \beta, \gamma), \quad (2)$$

where

$$\mathbf{T}(t_x, t_y, t_z) = \begin{pmatrix} 1 & 0 & 0 & t_x \\ 0 & 1 & 0 & t_y \\ 0 & 0 & 1 & t_z \\ 0 & 0 & 0 & 1 \end{pmatrix} \quad (3)$$

and

$$\mathbf{R}(\alpha, \beta, \gamma) = \mathbf{R}_z(\gamma) \cdot \mathbf{R}_y(\beta) \cdot \mathbf{R}_x(\alpha) = \begin{pmatrix} r_{11} & r_{12} & r_{13} & 0 \\ r_{21} & r_{22} & r_{23} & 0 \\ r_{31} & r_{32} & r_{33} & 0 \\ 0 & 0 & 0 & 1 \end{pmatrix}, \quad (4)$$

where $R_x(\alpha), R_y(\beta)$, and $R_z(\gamma)$ are rotations of α, β, *and* γ radians about the x-axis, y-axis and z-axis, respectively.

With

$$R_x(\alpha) = \begin{bmatrix} 1 & 0 & 0 \\ 0 & \cos\alpha & -\sin\alpha \\ 0 & \sin\alpha & \cos\alpha \end{bmatrix} \quad (5)$$

$$R_y(\beta) = \begin{bmatrix} \cos\beta & 0 & \sin\beta \\ 0 & 1 & 0 \\ -\sin\beta & 0 & \cos\beta \end{bmatrix} \quad (6)$$

$$R_z(\gamma) = \begin{bmatrix} \cos\gamma & -\sin\gamma & 0 \\ \sin\gamma & \cos\gamma & 0 \\ 0 & 0 & 1 \end{bmatrix} \quad (7)$$

$$\begin{aligned} r_{11} &= \cos\gamma\cos\beta \\ r_{12} &= -\sin\gamma\cos\alpha + \cos\gamma\sin\beta\sin\alpha \\ r_{13} &= \sin\gamma\sin\alpha + \cos\gamma\sin\beta\cos\alpha \\ r_{21} &= \sin\gamma\cos\beta \\ r_{22} &= \cos\gamma\cos\alpha + \sin\gamma\sin\beta\sin\alpha \\ r_{23} &= -\cos\gamma\sin\alpha + \sin\gamma\sin\beta\cos\alpha \\ r_{31} &= -\sin\beta \\ r_{32} &= \cos\beta\sin\alpha \\ r_{33} &= \cos\beta\cos\alpha \end{aligned} \quad (8)$$

Equation (1) is essentially a least squares optimization problem, which requires only determining the values of the six parameters $\alpha, \beta, \gamma, t_x, t_y$, and t_z. However, since α, β, and γ are the independent variables of a nonlinear trigonometric function in a rotation matrix R, we approach this nonlinear least squares problem with linearization in order to apply the linear least squares technique.

In each iteration when an angle $\theta \approx 0$, approximations $\cos\theta \approx 1$, $\sin\theta \approx \theta$, and $\theta^2 \approx 0$ can be used. Therefore, when $\alpha, \beta, \gamma \to 0$

$$\mathbf{R}(\alpha,\beta,\gamma)\approx\begin{pmatrix}1 & \alpha\beta-\gamma & \alpha\gamma+\beta & 0\\ \gamma & \alpha\beta\gamma+1 & \beta\gamma-\alpha & 0\\ -\beta & \alpha & 1 & 0\\ 0 & 0 & 0 & 1\end{pmatrix}$$
$$\approx\begin{pmatrix}1 & -\gamma & \beta & 0\\ \gamma & 1 & -\alpha & 0\\ -\beta & \alpha & 1 & 0\\ 0 & 0 & 0 & 1\end{pmatrix}=\hat{\mathbf{R}}(\alpha,\beta,\gamma) \quad (9)$$

We can now rewrite (1) as

$$\hat{M}_{opt}=\arg\min_{\hat{M}}\sum_i((\hat{M}\bullet p_i-q_i)\bullet n_i)^2 \quad (10)$$

Each $(\hat{M}\bullet p_i-q_i)\bullet n_i$ *in (10)* can be written as a linear expression of the six parameters $\alpha,\beta,\lambda,t_x,t_y,$ *and* t_z *:*

$$(\hat{M}\bullet p_i-q_i)\bullet n_i=\left(\hat{M}\bullet\begin{pmatrix}p_{ix}\\ p_{iy}\\ p_{iz}\\ 1\end{pmatrix}-\begin{pmatrix}q_{ix}\\ q_{iy}\\ q_{iz}\\ 1\end{pmatrix}\right)\bullet\begin{pmatrix}n_{ix}\\ n_{iy}\\ n_{iz}\\ 0\end{pmatrix} \quad (11)$$
$$=\left(n_{iz}p_{iy}-n_{iy}p_{iz}\right)\alpha+\left(n_{ix}p_{iz}-n_{iz}p_{ix}\right)\beta+$$
$$+\left(n_{iy}p_{ix}-n_{ix}p_{iy}\right)\gamma+n_{ix}t_x+n_{iy}t_y+n_{iz}t_z-$$
$$\left(n_{ix}q_{ix}+n_{iy}q_{iy}+n_{iz}q_{iz}-n_{ix}p_{ix}-n_{iy}p_{iy}-n_{iz}p_{iz}\right)$$

Given N pairs of point correspondences, we can arrange all $(\hat{M}\bullet p_i-q_i)\bullet n_i,\ 1\le i\le N$, into a matrix expression

$$E(R,t)=\sum_{i=1}^{N}\left(\left(Rp_i+t-q_i\right)^T n_i\right)^2=\|Ax-b\|^2, \quad (12)$$

where

$$x=(\alpha\quad\beta\quad\gamma\quad t_x\quad t_y\quad t_z)^T \quad (13)$$

$$b=\begin{bmatrix}n_{1x}q_{1x}+n_{1y}q_{1y}+n_{1z}q_{1z}-n_{1x}p_{1x}-n_{1y}p_{1y}-n_{1z}p_{1z}\\ n_{2x}q_{2x}+n_{2y}q_{2y}+n_{2z}q_{2z}-n_{2x}p_{2x}-n_{2y}p_{2y}-n_{2z}p_{2z}\\ \vdots\\ n_{Nx}q_{Nx}+n_{Ny}q_{Ny}+n_{Nz}q_{Nz}-n_{Nx}p_{Nx}-n_{Ny}p_{Ny}-n_{Nz}p_{Nz}\end{bmatrix} \quad (14)$$

and

$$A=\begin{bmatrix}a_{11} & a_{12} & a_{13} & n_{1x} & n_{1y} & n_{1z}\\ a_{21} & a_{22} & a_{23} & n_{2x} & n_{2y} & n_{2z}\\ \vdots & \vdots & \vdots & \vdots & \vdots & \vdots\\ a_{N1} & a_{N2} & a_{N3} & n_{Nx} & n_{Ny} & n_{Nz}\end{bmatrix} \quad (15)$$

with

$$\begin{aligned}a_{i1}&=n_{iz}p_{iy}-n_{iy}p_{iz}\\ a_{i2}&=n_{ix}p_{iz}-n_{iz}p_{ix}\\ a_{i3}&=n_{iy}p_{iz}-n_{ix}p_{iy}\end{aligned}, \quad (16)$$

which is a standard linear least-squares problem, and can be solved using SVD (singular value decomposition).

$$\hat{x}=\arg\min_x E(x)=\|Ax-b\|^2=(A^TA)^{-1}A^Tb. \quad (17)$$

Let $A=U\Lambda V^T$ be the SVD of A. The pseudo-inverse of A is defined as the matrix $A^{-1}=V\Lambda^{-1}U^T$, where Λ^{-1} is the matrix formed by taking the inverse of the non-zero elements of Λ (and leaving the zero elements unchanged). Then, rotation matrix $R(\alpha,\beta,\gamma)$ and translation matrix $T(t_x,t_y,t_z)$ can be computed from $\hat{x}$,the solution to the least-squares problem (17) is done. The procedure is fully explained in Algorithm 2.

Algorithm 2. *M = ICP(P,Q,M$_0$)*

M=M$_0$
while $\|M'\|>\in$ ***do***
  for $i=1:n$ ***do***
    $q_i=Mq_i$
  end for
  for $i=1:n$ ***do***
    $p_i=\text{FindClosetPoint}(P,q_i)$
  end for
    $p_m=\frac{1}{n}\sum p_i$
    $q_m=\frac{1}{n}\sum q_i$
  for $i=1:n$ ***do***
    $p_i'=p_i-p_m;q_i'=q_i-q_m$
  end for
  $[U,\Lambda,V]=SVD(\sum q_i'\otimes\sum p_i')$
  $R=UV^T$
  $t=p_m-Rq_m$
  $M'=\begin{bmatrix}R & t\\ 0 & 1\end{bmatrix}$
  $M=M'M$
end while
return M

At each iteration of the ICP algorithm, the standard nonlinear least square method is used to solve the relative position and posture changes that produce the minimum point-to-plane error. Then a three-dimensional rigid body transformation matrix is constructed from the linear least square solution.

The subsequent work is to transfer the positioning parameters of the point cloud registration to the fracture surgical robot system (such as the Taylor external frame), and through the reduction path planning, the system performs the reduction and fixation operations, as shown in Figure 4.

Figure 4
Surgical robot reduction and fixation of fracture site

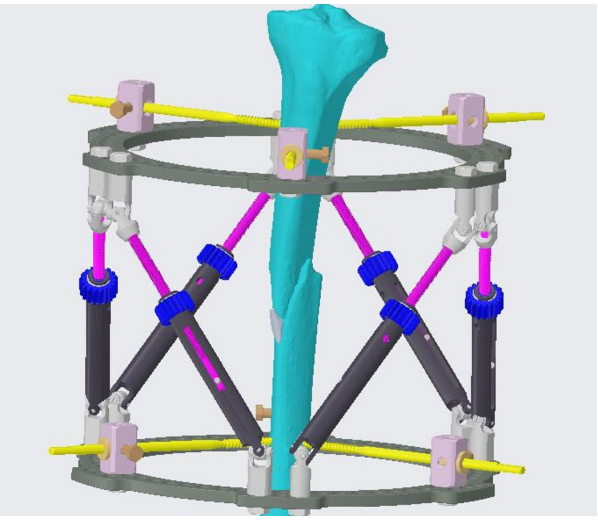

The reference system that describes the relative position of each structural part of the human body in space is usually composed of three planes: sagittal plane, frontal plane and horizontal plane.

Sagittal plane: The movement of dividing the body into left and right halves, forward and backward.

Coronal plane: Divides the body into front and back halves, moving side to side.

Horizontal plane: Cut the body into the upper and lower halves and twist the motion.

The system described in this paper, where the x, y, and z axes correspond to the transverse, coronal, and sagittal planes, respectively.

$R_x(\alpha), R_y(\beta)$, and $R_z(\gamma)$ are rotations of α, β, and γ radians about the x-axis, y-axis and z-axis, t_x, t_y, and t_z are the displacement on the x, y, and z axes, respectively. In this paper, the motion control parameters of the surgical robot are one-by-one corresponding to six parameters such as α, β, γ t_x, t_y, and t_z.

4. Result

Due to the difference in X-ray absorption degree caused by different tissue structures of the human body, the nature of tissues can be identified by CT value, and the unit of CT value is Hounsfield Unit (HU). The density of bone tissue is high, generally above 300HU. Figures 5-6 represent the 3D image reconstruction of the tibia from the 3-Matic Research software and our project, which consists of fragments 1-3, respectively. In this case, the CT value of the tibial shaft fracture site was high, and a threshold of 1200HU was set in the program to generate a 3D reconstruction model. As for the generated visual shapes, there is no significant difference between the 3-Matic Research software and our project. The three doctors believed that the tibial visible shape output by 3D reconstruction in this project could meet the clinical application requirements and be integrated with the subsequent registration algorithm to achieve virtual fracture reduction.

Figure 5
Reconstruction from 3-Matic

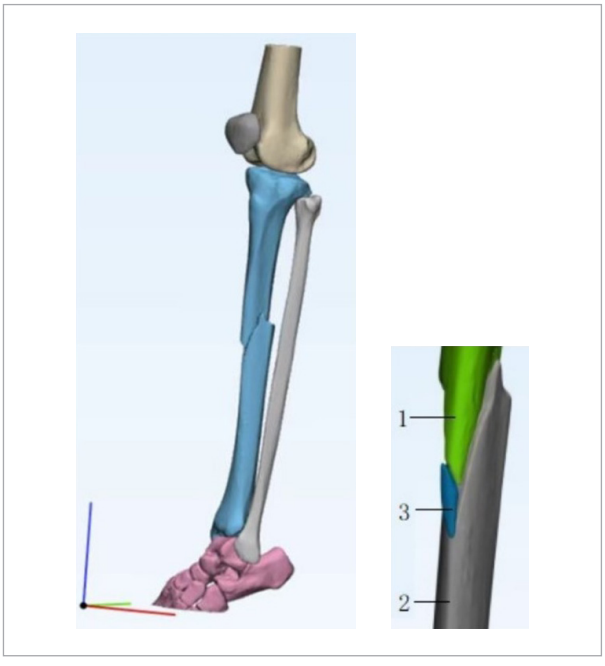

Figure 6
Reconstruction from our work

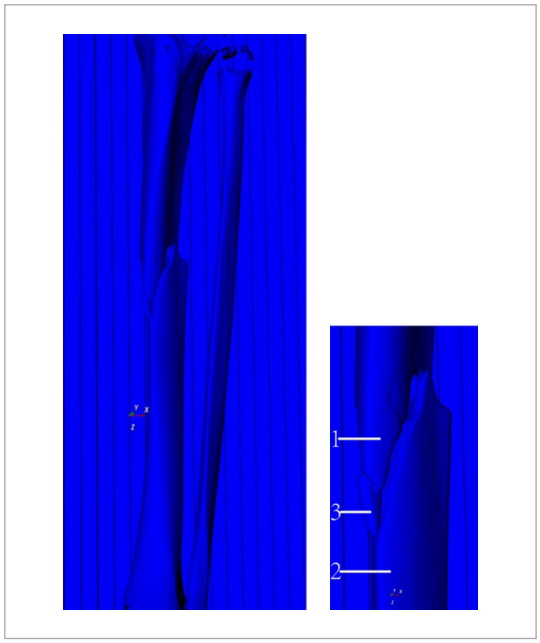

Table 1
Tibial Fracture No. 1 Fragment Surface Dimensions

Description	3-Matic Research	Our Project	Deviation (%)
Volume (mm3)	109172.3702	108626.5083	0.5%
Area (mm2)	32697.6110	32534.1230	0.5%

Table 2
Tibial Fracture No. 2 Fragment Surface Dimensions

Description	3-Matic Research	Our Project	Deviation (%)
Volume (mm3)	86102.9648	85672.4500	0.5%
Area(mm2)	23940.7108	23821.0073	0.5%

Table 3
Tibial Fracture No. 3 Fragment Surface Dimensions

Description	3-Matic Research	Our Project	Deviation (%)
Volume (mm3)	198.1217	197.1312	0.5%
Area (mm2)	228.5883	227.4455	0.5%

Tables 1-3 show the surface area and surface volume of each tibia fragment after 3D reconstruction from 3-Matic research software and the program of this project. The data in these tables show that our project and 3-Matic Research software are similar in the surface dimensions generated, with a deviation of less than 1%. The surface area and volume of bone segments 1 and 2 are large, representing the proximal and distal parts of tibial fractures. The No. 3 bone fragment is too small and does not require a reduction in actual clinical cases. The error processes involved in our method include CT scanning, 3D reconstruction, algorithm convergence, etc. As shown in Tables 1-3, the result error of 3D reconstruction is 0.5%. There may be some cumulative error. Nevertheless, after consulting with a surgeon (an expert in the field), these errors were deemed clinically acceptable.

Figure 7 shows the point cloud data acquired in the 3D reconstruction step. An intact point cloud and a locally enlarged view of the tibial fracture were established.

Figure 7
Generated fracture point cloud data: (a) An intact tibial fracture point cloud, (b) a Locally enlarged view of the fractured bone point cloud

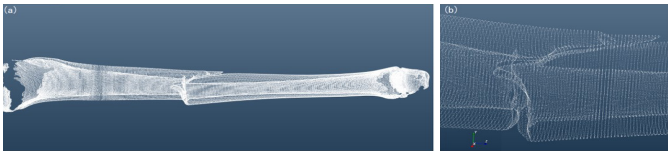

Figure 8
Identification results of bone fragmentation point set in fracture area (a case of female tibial oblique fracture): (a) Unseparated tibial fracture point cloud data, (b) Fracture point cloud data after separation, different bone segments are displayed in different colors, (c) Proximal point cloud of tibial fracture, and (d) Distal point cloud of tibial fractures

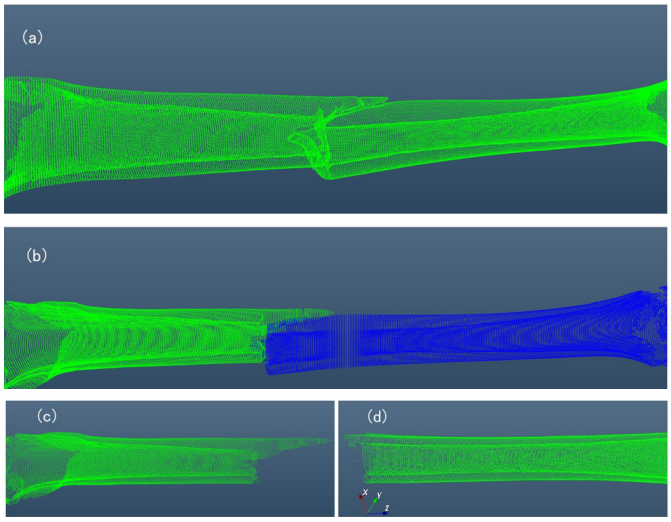

The algorithm described in the methods section has been successfully applied to identify tibia fractures in the area, as shown in Figure 8.

The tibial bone is mainly composed of cortical bone and cancellous bone, in which the cancellous bone has a lower strength and is located at both ends of the tibia, while the cortical bone has a higher strength and is located in the middle of the tibia. The adjustment of CT values presents different imaging effects, so there is a cavity phenomenon at both ends of the tibia in this paper. This is a clinical case of a fracture of the middle tibia, and the cavitation phenomenon does not affect the accuracy of virtual reduction.

The CT stack contains an oblique fracture of the tibia, and 637 slices form it with dimensions 230*230 mm and 0.7999 mm spacing. Table 4 summarizes the parameters of the CT stack used as input for the experiment.

For the reduction of tibial shaft fractures, the method based on the combination of NDT and ICP performed well. As shown in Figure 9(a), there were suitable matches between bone fragments. The three-dimensional reconstruction after fracture reduction is in Figure 9(b).

Table 4
The Data Specification of the Experiment

Category	Slice Quantity	Format Size(mm)	Slice Spacing
Tibia(female)	637	230*230	0.7999

Figure 9
The result of the proposed algorithm processing: (a) The registration results of point cloud data, (b) Three-dimensional reconstruction model of tibial fracture after registration

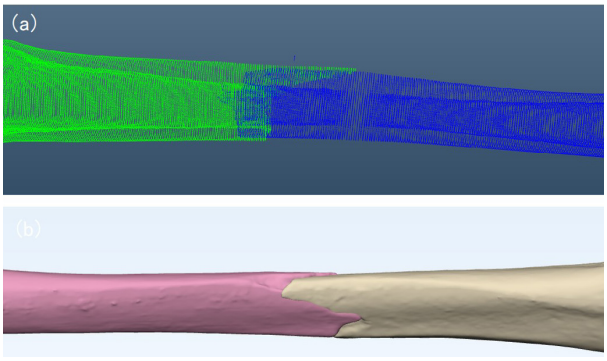

The three steps involved in the experimental algorithm, namely 3D reconstruction, broken bone identification, and point cloud registration, are evaluated for their efficiency, and the running time is given in Table 5.

Table 5
Running time at each step

#vertices		Time (in a sec)				
Fragment 1	Fragment 2	Reconstruction	Filter	Segmentation	Registration	Total
10070	24136	24.635	0.384	22.712	1.918	48.649

It takes approximately 48s to run the entire process using Visual Studio 2019 on a workstation equipped with an Intel(R) Core(TM) I7-7820HQ CPU at 2.9ghz and an NVIDIA Quadro M1200.

5. Discussion

In virtual fracture reduction, semi-automatic methods require the user to identify and pair points on the fracture surfaces to be reduced by minimizing the squared sum of distances between the points. However, since there are usually no distinguished anatomical landmarks on the fracture surface interface, the localization and pairing of the matching points is also errorprone and time-consuming. Consequently, automatic virtual bone fracture reduction is highly desirable. Automated methods are usually done by inputting geometric models of fracture fragments or raw CT scan data. It identifies the point cloud data in each fracture fragment, performs a 3D reconstruction, and aligns them by iterating the nearest point rigid registration. The resulting transformation is applied to the fracture fragment to produce the position and orientation of the reduced fracture. An automated approach has been proposed, from bone segmentation to 3D reconstruction, to identification of fractured bones, and finally to registration. Therefore, it applies to real bones from clinical studies rather than artificial bones.

3D image reconstruction is a challenge because the model of long human bones is very different from other models. From the point of view of medical diagnosis, it is unnecessary to know the exact reduction details excessively. In clinical practice, one of the most important purposes of fracture fixation is to reduce the length and alignment of the bone, which can restore the function of the long bone. The MC method can meet the requirements of accuracy and high efficiency. The tibial model reconstructed by the MC algorithm is similar to the model obtained by 3-mathematical medical software. For the quantitative analysis of the two models, the data of the tibia model reconstructed by the MC algorithm can be saved in stereolithography (STL) format. Then the files can be imported into Geomagic for comparison.

A method of automatic identification of fractured bones is proposed in this paper. Unlike other methods presented in references [4, 17, 21], our approach avoids calculating the curvature of point clouds and manually determining the initial position among fracture segments, which is tedious and a waste of time. Sometimes, due to the low intensity of trabecular tissue, it is even impossible to segment it from CT images with the parameters of the CT scanner. Tibia consists of cortical bone and cancellous bone, among which cortical bone has high strength and is not easy to deform, cancellous bone has low strength, and tissue deformation is easy to occur in fracture. When there is a mixture of cortical and cancellous bone in the fracture, the surgeon usually extracts the point cloud information of the bone tissue by setting multiple strength values, and gradually calculates the reduction information of the fracture.

In terms of registration, compared with most previous methods, our method combines the respective advantages of NDT coarse registration algorithm and improved ICP fine registration algorithm. In the algorithm program, the threshold of distance parameter is set to determine whether the initial alignment is necessary for different fracture types. In particular, in the presence of crush and rotation injuries, bone fragments move or rotate significantly relative to their original position. The experimental results show that the method is robust when there is a small displacement between the initial locations of broken bone fragments, and the initial alignment has no significant effect on the reduction accuracy in such cases. However, due to insufficient clinical data, this method has not been implemented in high-energy comminuted fractures where large displacements or rotations require initial registration.

Our experiments used a case from actual tibial fractures. On the one hand, fewer experimental samples were a recurring problem in the literature [29, 6, 18]. Based on an actual situation, obtaining CT of cases where fractures can be reduced without fixation is challenging. On the other hand, there were no prescribed criteria to evaluate the accuracy of fracture reduction results. ICP-based registration methods can test the accuracy of the final alignment of the fracture surface by the mean squared error (MSE) [3]. It is mentioned in the supplementary reference [14] that the mean robot fracture reduction time is 4 minutes 13 seconds, compared with the total virtual reduction time of 48 seconds for the method proposed in this paper without involving robot operation, which indicates that it is more likely to shorten the robot reduction time under this approach. In addition, the fracture reduction method described in this paper uses the surface contour normal vector for axial evaluation, hiding points perpendicular to the axis on the surface of the point cloud. The experimental results show no prominent contour in the area after reduction, which is only limited to long bone shaft fractures.

Computational efficiency will significantly affect preoperative planning and intraoperative surgery, which is important in evaluating the feasibility of the scheme in clinical practice. The proposed method is computationally demanding, but it can be implemented in a reasonable time through graphic processing unit (GPU) acceleration. The total planning time mainly depends on the resolution of CT images, the fragments' size, and the fractures' complexity. This experiment's computational workload is lower than simple fractures with tiny pieces.

6. Conclusion

The proposed system is a complete preoperative planning system for fracture reduction, which mainly includes three steps: 3D reconstruction, broken bone identification, and alignment and registration. The

whole system has only a small amount of interaction. The three-dimensional reconstruction of the fracture site is beneficial to the early medical diagnosis, the planning of the treatment plan, and the training of the trainee, especially for understanding complex comminuted fractures. Postoperative reconstruction can help inform the outcome of the surgery and improve treatment.

The proposed k-nearest neighbor clustering method completes the identification of two bone segments without calculating the curvature of the fracture area or placing seed points. The registration method of this paper has been successfully applied to tibial fracture cases. The obtained results showed that the tested clinical cases achieved successful fracture reduction due to no visible overlap or gaps between the fragments. The tests show that combining the NDT algorithm and the improved ICP algorithm is suitable for situations where there is a slight movement of the initial position of the bone fragments. In addition, the operation of the entire system is time-sensitive and only takes a few minutes to implement. Despite these results, clinical studies are needed to determine whether the approach improves preoperative planning for fracture reduction.

On the basis of single tibial fracture specimens, the method has achieved good reduction effect and is suitable for the reduction of long bone fractures. However, there may be some specific areas or cases that were not considered in this study. It is considered necessary to further test the method in further practical clinical cases.

Abbreviations

CT	Computed tomography
MC	Marching cube
KD	K-dimensional
ICP	Iterative closest point
3D	Three-dimensional
RANSAC	Random sample consistency
NDT	Normal distributions transform
KNN	K-nearest neighbor
MSE	Mean squared error
STL	Stereolithography
VTK	Visualization toolkit
SSM	Statistical shape model
SPM	Statistical pose model
GCP	Good clinical practice
ICH-GCP	Guideline for Good Clinical Practice of the International Conference on Harmonisation
GPU	Graphic processing unit
HU	Hounsfield unit

Conflict of Interest Statement

The authors declare no known competing financial interests or personal relationships that could have appeared to influence the work reported in this paper.

Funding

This Study was supported by the Zhejiang Science and Technology Plan Project-National Key Research and Development Program of China (Grant No. 2019C03075).

Data Availability Statement

The datasets used and/or analyzed during the current study are available from the corresponding authors on reasonable request.

Authors' Contributions

Qinghua Yang, Yi Xun, Xinxing Zhang were the principal investigators of the study. Qinghua Yang, Xinxing Zhang and Jun Qian participated in the design of the study and performed the data analysis. Qinghua Yang obtained grant funding and Jun Qian obtained local ethics approval. Xinxing Zhang and Yi Xun wrote the program code. Xinxing Zhang wrote the manuscript and Yunsheng Mao put forward suggestions for revision. Yingqi Zhang and Juncai Ye contributed to the acquisition and interpretation of the data and analyses. All authors read and approved the final manuscript.

References

1. Arumugam, S., Ranganathan, R., Narayanasamy, V. K. Virtual Registration of Comminuted Bone Fracture and Preoperative Assessment of Reconstructed Bone Model Using the Procrustes Algorithm Based on CT Dataset. Proceedings of the Institution of Mechanical Engineers, Part H: Journal of Engineering in Medicine, 2024. https://doi.org/10.1177/09544119231221192
2. Buschbaum, J., Fremd, R., Pohlemann, T., Kristen, A. Computer-Assisted Fracture Reduction: A New Approach for Repositioning Femoral Fractures and Planning Reduction Paths. International Journal of Computer Assisted Radiology and Surgery, 2015, 10(2), 149-159. https://doi.org/10.1007/s11548-014-1011-2
3. Chowdhury, A. S., Bhandarkar, S. M., Robinson, R. W., & Yu, J. C. Virtual Multi-Fracture Craniofacial Reconstruction Using Computer Vision and Graph Matching. Comput Med Imaging Graph, 2009, 33(5), 333-342. https://doi.org/10.1016/j.compmedimag.2009.01.006
4. Chowdhury, A. S., Bhandarkar, S. M., Robinson, R. W., Yu, J. Virtual Craniofacial Reconstruction from Computed Tomography Image Sequences Exhibiting Multiple Fractures. In 2006 International Conference on Image Processing, IEEE, 2006, 1173-1176. https://doi.org/10.1109/ICIP.2006.312766
5. Deng, Z., Jiang, J., Liu, H., Cheng, Z., Huang, R., Zhang, W. A Data-Driven Approach for Assembling Intertrochanteric Fractures by Axis-Position Alignment. IEEE Access. 2020, 8, 137549-137563. https://doi.org/10.1109/ACCESS.2020.3012047
6. Furnstahl, P., Szekely, G., Gerber, C., Hodler, J., Snedeker, J. G., Harders, M. Computer-Assisted Reconstruction of Complex Proximal Humerus Fractures for Preoperative Planning. Medical Image Analysis, 2010, 16(3), 704-720. https://doi.org/10.1016/j.media.2010.07.012
7. Han, R., Uneri, A., Ketcha, M., Vijayan, R., Sheth, N., Wu, P. Multi-Body 3D-2D Registration for Image-Guided Reduction of Pelvic Dislocation in Orthopaedic Trauma Surgery. Physics in Medicine & Biology, 2020, 65(13), 135009. https://doi.org/10.1088/1361-6560/ab843c
8. Han, R., Uneri, A., Vijayan, R. C., Wu, P., Vagdargi, P., Sheth, N. Fracture Reduction Planning and Guidance in Orthopaedic Trauma Surgery via Multi-Body Image Registration. Med Image Anal, 2021, 68, 101917. https://doi.org/10.1016/j.media.2020.101917
9. Han, R., Uneri, A., Wu, P., Vijayan, R. C., Vagdargi, P., Ketcha, M.D., Sheth, N., Vogt, S., Kleinszig, G., Osgood, G. M., Siewerdsen, J. H. Multi-Body Registration for Fracture Reduction in Orthopaedic Trauma Surgery. Proceedings of SPIE 11315, Medical Imaging 2020: Image-Guided Procedures, Robotic Interventions, and Modeling, 16 March 2020, 113150F. https://doi.org/10.1117/12.2549708
10. Hernandez, D., Garimella, R., Eltorai, A. E. M., Daniels, A. H. Computer-Assisted Orthopaedic Surgery. Orthopaedic Surgery, 2017, 9(2), 152-158. https://doi.org/10.1111/os.12323
11. Jiménez-Delgado, J. J., Paulano-Godino, F., PulidoRam-Ramírez, R., Jiménez-Pérez, J. R. Computer-Assisted Preoperative Planning of Bone Fracture Reduction: Simulation Techniques and New Trends. Medical Image Analysis, 2016, 30, 30-45. https://doi.org/10.1016/j.media.2015.12.005
12. Kronman, A., Joskowicz, L. Automatic Bone Fracture Reduction by Fracture Contact Surface Identification and Registration. In 2013 IEEE 10th International Symposium on Biomedical Imaging, IEEE, 2013, 246-249. https://doi.org/10.1109/ISBI.2013.6556458
13. Liu, B., Zhang, S., Zhang, J., Xu, Z., Chen, Y., Liu, S. A Personalized Preoperative Modeling System for Internal Fixation Plates in Long Bone Fracture Surgery-A Straightforward Way from CT Images to Plate Model. The International Journal of Medical Robotics and Computer-Assisted Surgery, 2019, 15(5), e2029. https://doi.org/10.1002/rcs.2029
14. Low, K. L. Linear Least-Squares Optimization for Point-to-Plane ICP Surface Registration. Chapel Hill, University of North Carolina, 2004, 1-3.
15. Luque-Luque, A., Perez-Cano, F. D., Jimenez-Delgado, J. J. Complex Fracture Reduction by Exact Identification of the Fracture Zone. Med Image Anal, 2021, 72, 102120. https://doi.org/10.1016/j.media.2021.102120
16. Magnusson, M. The Three-Dimensional Normal-Distributions Transform: An Efficient Representation for Registration, Surface Analysis, and Loop Detection. Örebro Universitet, 2009.
17. Moghari, M. H., Abolmaesumi, P. Global Registration of Multiple Bone Fragments Using Statistical Atlas Models: Feasibility Experiments. 30th Annual International Conference of the IEEE Engineering in Medicine and Biology Society, 2008. https://doi.org/10.1109/IEMBS.2008.4650429
18. Okada, T., Iwasaki, Y., Koyama, T., Sugano, N., Chen, Y. W., Yonenobu, K. Computer-Assisted Preoperative Planning for Reduction of Proximal Femoral Fracture Using 3-D-CT Data. IEEE Transactions on Biomed-

ical Engineering, 2009, 56(3), 749-759. https://doi.org/10.1109/TBME.2008.2005970

19. Paulano-Godino, F., Jimenez-Delgado, J. J. Identification of Fracture Zones and Its Application in Automatic Bone Fracture Reduction. Computer Methods and Programs in Biomedicine. 2017, 141, 93-104. https://doi.org/10.1016/j.cmpb.2016.12.014
20. Picard, F., Deakin, A. H., Riches, P. E., Deep, K., Baines, J. Computer-Assisted Orthopaedic Surgery: Past, Present, and Future. Med Eng Phys, 2019, 72, 55-65. https://doi.org/10.1016/j.medengphy.2019.08.005
21. Poelert, S., Valstar, E., Weinans, H., Zadpoor, A. A. Patient-Specific Finite Element Modeling of Bones. Proceedings of the Institution of Mechanical Engineers, Part H: Journal of Engineering in Medicine, 2013, 227(4), 464-478. https://doi.org/10.1177/0954411912467884
22. Purnama, I. L. I., Tontowi, A. E., Herianto, H. 3D Image Reconstruction with Single-Slice CT Using Improved Marching Cube Algorithm. In 2019 International Biomedical Instrumentation and Technology Conference, 2019, l, 84-87. https://doi.org/10.1109/IBITeC46597.2019.9091687
23. Rusinkiewicz, S., Levoy, M. Efficient Variants of the ICP Algorithm. In Proceedings Third International Conference on 3-D Digital Imaging and Modeling, 2001, 145-152. https://doi.org/10.1109/IM.2001.924423
24. Vlachopoulos, L., Szekely, G., Gerber, C., Furnstahl, P. A Scale-Space Curvature Matching Algorithm for the Reconstruction of Complex Proximal Humeral Fractures. Medical Image Analysis, 2018, 43, 142-156. https://doi.org/10.1016/j.media.2017.10.006
25. Westphal, R., Winkelbach, S., Wahl, F., Gösling, T., Oszwald, M., Hüfner, T., Krettek, C. Robot-Assisted Long Bone Fracture Reduction. The International Journal of Robotics Research, 2009, 28(10), 1259-1278. https://doi.org/10.1177/0278364909101189
26. Willis, A., Anderson, D., Thomas, T., Brown, T., Marsh, J. L. 3D Reconstruction of Highly Fragmented Bone Fractures. In Medical Imaging 2007: Image Processing, 2017, 6512, 595-604. SPIE. https://doi.org/10.1117/12.708683
27. Winkelbach, S., Rilk, M., Schönfelder, C., Wahl, F. M. Fast Random Sample Matching of 3D Fragments. Pattern Recognition: 26th DAGM Symposium, Tübingen, Germany, August 30-September 1, 2004. Proceedings 26, Springer Berlin Heidelberg, 2004, 129-136. https://doi.org/10.1007/978-3-540-28649-3_16
28. Winkelbach, S., Westphal, R., Goesling, T. Pose Estimation of Cylindrical Fragments for Semi-Automatic Bone Fracture Reduction. In: Michaelis, B., Krell, G. (eds) Pattern Recognition. DAGM 2003. Lecture Notes in Computer Science, 2003, 2781. https://doi.org/10.1007/978-3-540-45243-0_72
29. Zhou, B., Willis, A., Sui, Y., Anderson, D., Thomas, T., Brown, T. Improving Inter-Fragmentary Alignment for Virtual 3D Reconstruction of Highly Fragmented Bone Fractures, Proc. SPIE 7259, Medical Imaging 2009: Image Processing, 27 March 2009, 725934. https://doi.org/10.1117/12.810967